In situ photopatterning of cell laden biomaterials for spatially organized 3D cell cultures in a microfluidic chip

Jennifer Ortiz-Cárdenas[a], Jonathan M. Zatorski[a], Alyssa N. Montalbine[a], Abhinav Arneja[b]
Chance John Luckey[b], Rebecca R. Pompano[a,c]*

[a]Department of Chemistry
University of Virginia
PO BOX 400319
Charlottesville, VA, USA 22904
Tel: 434-982-1825

[b]Department of Pathology
University of Virginia
Charlottesville, VA, USA 22904

[c]Department of Chemistry
Carter Immunology Center
University of Virginia
PO BOX 400319
Charlottesville, VA, USA 22904

*Corresponding author: rpompano@virginia.edu

Abstract

Micropatterning techniques have enabled the use of 3D cell cultures to recreate tissue-level behavior such as hypoxia or signaling gradients, but their integration with microfluidics has been limited. To access complex, non-linear and concentric geometries seen in vivo and in high-throughput culture arrays, we developed an in-situ micropatterning strategy that integrated photolithography of crosslinkable, cell-laden hydrogels with a simple microfluidic housing. By shining 405 nm light through a photomask containing the desired design, we patterned 3D cultures directly in a 130-μm deep microfluidic chamber. As a model system, we used thiol-ene step growth polymerization with thiol-modified gelatin (GelSH) and PEG-norbornene linker; the technology was also applicable to other photo-crosslinkable chemistries, including gelatin methacryloyl (GelMA) and gelatin norbornene (GelNB) with PEG-thiol linker. The on-chip patterning strategy generated 3D cultures that were self-standing and that could be combined using serial photomasks. The method consistently generated features as small as 100 μm in diameter, and shared, non-linear boundaries between cultures were readily achieved. The modularity of the platform meant that designs were interchangeable in the same microfluidic housing, without requiring new master fabrication. As a proof-of-principle, a fragile cell type, primary human T cells, were patterned in varied geometries. Cells were patterned with high regional specificity and viability remained high. We expect that this technology will enable researchers to organize 3D cultures into geometries that were previously difficult to obtain, granting access to biomimetic tissue organizations and 3D-cultured microarray formats.

Introduction

Micropatterned cell cultures have become valuable tools to study fundamentals of cell and tissue behavior, enabling questions regarding cell-cell and cell-matrix interactions and the generation of patterned arrays of cell cultures for high-throughput analyses.[1,2] Whereas optimization of 3D cultures traditionally focuses on the mechanical and biochemical properties of the cell culture matrix, the spatial arrangement of cell-laden 3D culture matrices offers an additional point of control to increase the biomimicry and utility of engineered tissues. For example, micropatterned 3D cultures have been used to replicate emergent tissue-level properties such as tissue hypoxia,[3,4] cell migratory and homing activity,[5,6] formation of signaling gradients,[7,8] and to form cell multi-arrays for high-throughput assays.[9–11] However, existing technologies are limited in their ability to create closely abutting, non-linear, cell-laden structures under fluidic control, and thus cannot fully replicate the complex spatial organization of native tissues or allow full freedom of high-throughput array design.

Current micropatterning techniques for 3D cultures include soft-lithography (microcontact printing and molding), bioprinting, and photolithography. Soft-lithography relies on elastomeric stamps or molds to promote selective cell or matrix adhesion,[12] directly cast 3D matrices[13,14]. Similarly, a newly developed method combines molds and surface tension for layer-by-layer patterning.[15] These methods are simple to use, but require multi-step fabrication of new stamps or molds for each pattern. In contrast, modern bioprinting allows for rapid prototyping of biomaterials in varied patterns based on digital designs, and can generate self-standing 3D cultures at the ~ mm length scale, with no need of physical supports. However, requirements for specific viscosities and surface tensions in extruded hydrogels restrict the options for the culture matrix.[16,17] On the other hand, photolithography uses light to transfer designs from a photomask to a photo-crosslinkable culture matrix to generate self-standing 3D cultures. Photolithography may offer higher spatial resolution than extrusion-based printing of bioinks.[18,19] A significant advantage of this method is the ability to modulate the mechanical properties of the hydrogel, e.g.

to match those of a particular tissue, by optimizing the chemical composition of the gel and dose of light, regardless of viscosity. Due to the risk of phototoxicity, photopatterning has been primarily used to pattern hydrogels without cells or limited to patterning hardy cell lines.[6,20–25] Photolithography is most commonly used to pattern hydrogels onto coverslips or other substrates that are rarely integrated with a flow control system.[26–29]

Integration of 3D cultures with fluidic control systems, particularly microfluidics, is often advantageous to control the microenvironment of the culture, but options for doing so are limited. While 3D cultures may be patterned off-chip and subsequently loaded into a microfluidic device, the alignment process may induce mechanical damage, particularly if there is a mismatch between the height of the microchamber and the culture. Therefore, methods for direct micropatterning of 3D cultures inside microfluidic chips have been developed, primarily by taking advantage of laminar flow and/or physical support structures. Patterns achieved through laminar flow are highly linear, producing well-controlled lanes of hydrogel.[30–33] Micropillars and other physical support structures allow more flexibility by patterning via surface tension, but typically also produce linear or gently curved boundaries.[34] These patterning strategies struggle to generate free-standing islands, concentric features, or two or more closely abutting cultures. In addition, patterning largely relies on pre-determined chip geometries, which means changes to the organization of the 3D culture may require time-consuming new master fabrication. In-situ photolithography overcomes these limitations, and has been used to coat microfluidic channels,[31] create monolayers of hydrogel onto which cells are later seeded,[35] and to create free-floating microstructures with and without cells for collection downstream.[36,37] Recently, on-chip photolithography was used to create cell-laden micropillar arrays and organized tumor-on-chip cultures.[6,9,24] However, photopatterning of more complex, non-linear, self-standing 3D cultures within a microfluidic chip remains a challenge, particularly with fragile primary cells.

In considering on-chip photopatterning of cell-laden hydrogels, the chemistry of the biomaterial was a significant factor in mitigating photo- or chemical-induced toxicity. In the

presence of a suitable photoinitiator and exposure to UV or violet light, methacrylate- and methacrylamide-functionalized biomaterials undergo rapid chain growth polymerization.[38] This methacryloyl-based polymerization is common, but it is severely inhibited by oxygen, leading to long and potentially toxic light exposures in the oxygen-rich culture matrix and oxygen-permeable microfluidic devices. Recently, thiol-norbornene (thiol-ene) chemistry was established as an alternative to methacryloyl-based crosslinking.[39,40] When exposed to blue light in the presence of a suitable photointiator and a norbornene-terminated linker, thiol-functionalized biomaterials form thioether bonds via thiol-ene step growth polymerization. This reaction is significantly faster and less toxic than chain-growth polymerizations because it is not inhibited by oxygen and even consumes reactive oxygen species.[40,41] Norbornene-modified biomaterials have been used successfully to encapsulate immortalized cell lines[40,42,43] and human mesenchymal stem cells[41] and may have potential for use with other fragile primary cells as well.

Here, we developed a user-friendly method to pattern 3D cell cultures into customizable, free-standing structures under fluidic control, by combining photolithography and photo-crosslinkable hydrogels within microfluidic devices. The stiffness of the hydrogels was tuned to fall within that of typical soft tissues and characterized via photo-rheology. We determined the resolution and robustness of the patterning method under varied conditions, and tested its versatility to generate complex geometries via sequential photomasks. Finally, we established its use for in-situ photo-patterning of sensitive primary cells, human T cells and murine splenocytes, and tested the spatial specificity of patterning as well as its impact on cell viability.

Results & Discussion

I. Gelation Chemistry and Matrix Optimization

To develop a photopatterning method for 3D culture inside a microfluidic device, we started by identifying matrix components, gelation chemistry, and wavelength of light to support cell viability and function. For simplicity, we selected a gelatin backbone. As a naturally-derived

material, gelatin provides cell adhesion (RGD) motifs and protease cleavage sites[44] and eliminates the need to dope in other materials for this purpose. Inclusion of cells in the hydrogel precursor meant that the potential toxicity of both the cross-linking chemistry and the light exposure had to be minimized. Thiol-modified gelatin (GelSH) was used to access biocompatible thiol-ene chemistry (**Fig. 1a**). An 8-arm PEG-norbornene (PEG-NB) was selected as the linker; multi-arm linkers form stiffer hydrogel networks than dual-arm equivalents at a given dose of light exposure,[41] which for our purposes helped reduce exposure time and thus photo-toxicity. GelSH is available commercially and is complimentary to GelNB materials that have been described previously for 3D cell culture.[40,41,45] Finally, the photo-initiator lithium phenyl-2,4,6-trimethylbenzoylphosphinate (LAP) was chosen due to its ability to absorb blue light (405 nm).[46] This wavelength is less cytotoxic to cells than the UV light (365 – 385 nm) that is required by more common photoinitiators such as Irgacure-2959. In the GelSH – PEG-NB system, both the protein and the PEG linkers are multifunctional, allowing branching to occur during polymerization to form an organized hydrogel network (**Fig. 1a**).

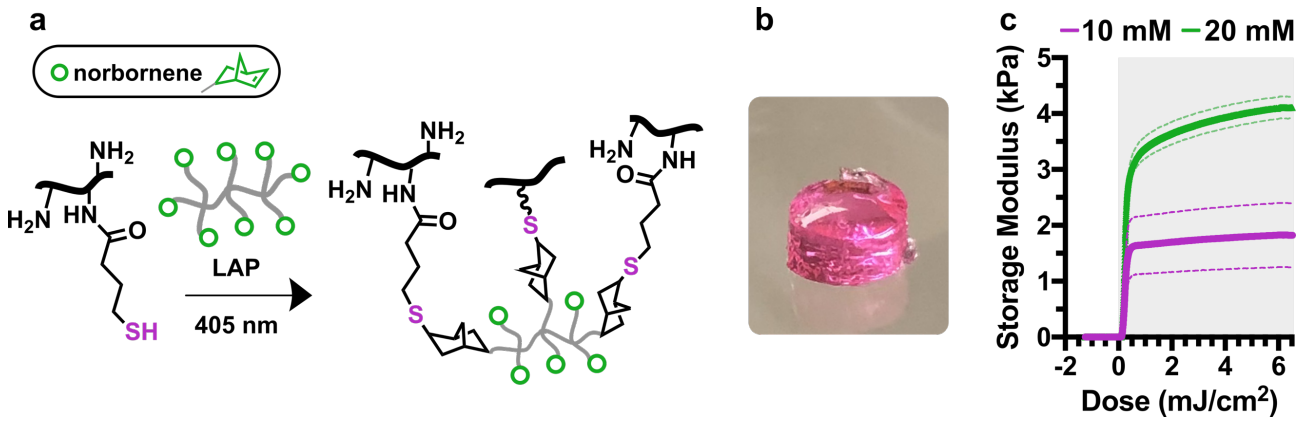

Fig. 1 Hydrogel chemistry and matrix optimization. (a) Reaction scheme of GelSH (black, thiol in magenta) with an 8-arm PEG-norbornene linker (grey, NB in green), catalyzed by the photoinitiator LAP and 405 nm light. (b) Photo of a puck of NHS-rhodamine-labeled GelSH after gelation in a 5 mm mold. (c) Rheometry measurements of the stiffness of the hydrogel during UV-curing *in situ*. Legend indicates the concentration of norbornene (8 mol norbornene per 1 mol PEG-NB). Lines show mean (solid) and std deviation (dashed), n = 3 technical replicates. Grey shading indicates the period when the light was turned on.

As expected, the GelSH – PEG-NB system formed self-supporting hydrogels when exposed to 405 nm light in the presence of LAP (**Fig. 1b**). The concentration of linker in the hydrogel was optimized to produce a stiffness in the range of 120 – 3000 Pa, to match of that typical soft tissues such as brain[47] and lymph nodes.[48,49] When rheology was performed during constant light exposure at 50 mW/cm^2 (5 % w/v GelSH; 3.4 mM LAP), gelation began immediately, with a rapid rise in storage modulus that began to level off in < 15 sec (**Fig. 1c**). A suitable stiffness of ~1500 Pa was achieved using 10 mM norbornene (1.25 mM PEG-NB) at all doses > 0.75 mJ/cm^2, and we used this linker concentration and range of light dose in subsequent experiments on-chip.

II. Device Design and Micropatterning Process

Having established a suitable gelation chemistry, we designed a simple and robust microfluidic housing for the patterned 3D cultures. The device was constructed from a thin layer of polydimethylsiloxane (PDMS) that was irreversibly bonded to a glass coverslip (**Fig. 2a**). PDMS

is a well characterized, gas-permeable polymer that has been successfully used for many on-chip cell culture applications, is readily silanized to control surface chemistry, and is transparent for photo-crosslinking and optical imaging.[50] For this work, the microchamber was designed with a 130-μm depth, sufficient to mimic a 3-dimensional tissue structure, and a 4.4-mm diameter at its widest point to provide sufficient surface area for complex patterns. These dimensions could be tailored readily in the future for specific applications. The chamber was tapered at each end to facilitate smooth filling.[51] In order to covalently anchor the patterned, norbornene-bearing hydrogel to the surface of the chip, the interior of the device was oxidized in a plasma cleaner and functionalized with a thiol-terminated silane (**Fig. 2b**). It was critical not to over-treat the PDMS surface with oxygen plasma, which caused cracks in the PDMS that templated defects in the hydrogel (Fig. S1).[52]

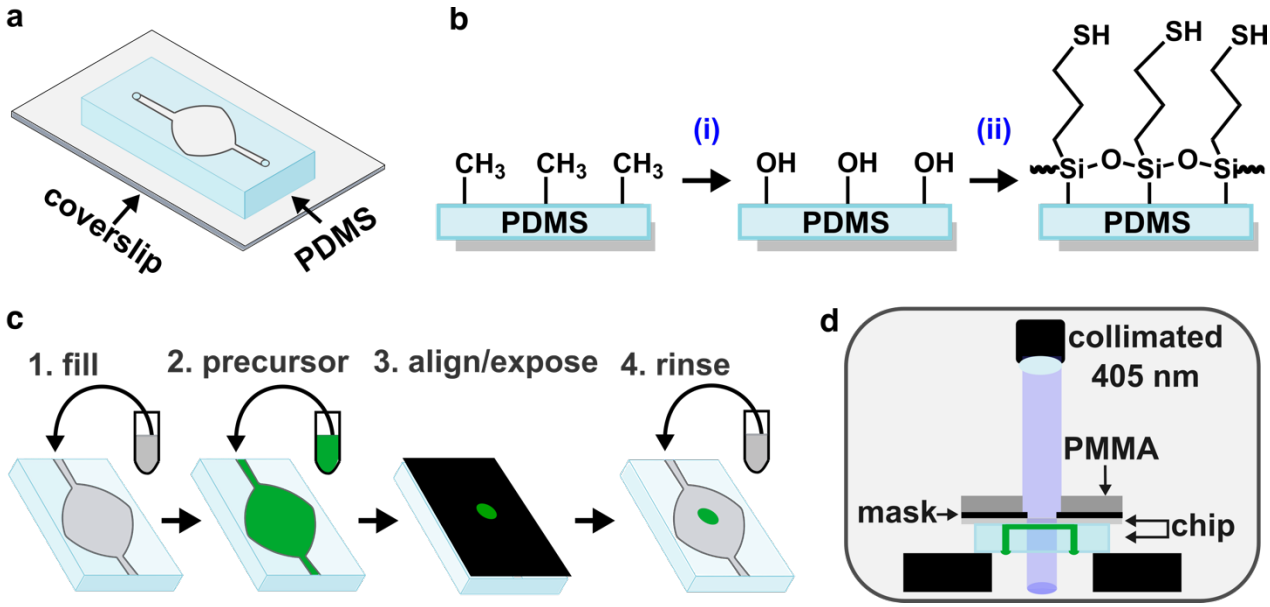

Fig. 2 Photo-patterning set-up and process. (a) Schematic of chip: thin layer of PDMS bonded to a glass coverslip. (b) Surface functionalization of PDMS. The methyl surface was (i) activated via oxidation with air plasma, followed by (ii) silanization using thiol-terminated silane. (c) Stepwise schematic of patterning process: 1) The chip was filled with buffer (grey), and 2) the buffer was displaced by precursor (green). 3) The photomask with desired design was aligned to the coverslip side of the chip, supported with a rigid polymer backing (PMMA), clamped (not shown for clarity), and exposed. 4) Unreacted material was removed with a buffer rinse. If needed, the process was repeated with a different precursor to add additional structures. (d) Schematic of photo-patterning set up. The chip was placed upside down on top of two support layers (black) to suspend it below the collimated light source. The channels and chamber of the chip are shown filled with precursor (green).

The patterning process consisted of four steps (**Fig. 2c**): After sterilization, the device was pre-wet with phosphate-buffered saline (PBS), filled with a precursor solution (e.g. GelSH, the PEG-NB linker, LAP, and the first population of cells) and sealed off to prevent air entry. The chip was placed briefly on a cooling stage to lower the temperature and ensure consistent gelation. Next, the photo-mask was aligned against the coverslip of the chip (Fig. S2), and the chip was placed upside down below a collimated 405 nm LED light source and exposed (**Fig. 2d**). Under these conditions, we found that a 2.25 mJ/cm^2 dose of light provided reproducible on-chip gelation. Finally, the inlet was unplugged, and unreacted precursor was removed by flowing

PBS, leaving only the patterned culture. The process was sequentially repeated with additional precursor solutions, e.g. containing different material compositions or different populations of cells. Once all patterning steps were completed, culture media was flowed into the chip and transferred to a cell culture incubator for continued culture.

III. **Resolution and robustness of on-chip photolithography**

The resolution and fidelity of patterning thick hydrogels by on-chip photolithography is expected to be limited by scattering of the incoming light and by diffusion of reactive species.[25] We tested the resolution and the agreement between the target and experimental dimensions by using photomasks with circular features (100 to 900 μm in diameter) to pattern the GelSH – PEG-NB hydrogel on-chip (**Fig. 3a**). First, chips prepared with a thin glass coverslip (0.15 mm thickness) were filled with precursor, exposed, rinsed with PBS to remove un-crosslinked material, and imaged to determine the dimensions of the freshly patterned structures (**Fig. 3b, top**). The chips then were placed in an incubator for thirty minutes without fluid flow, rinsed once more, and imaged again to determine the extent to which the dimensions had changed either due to swelling or defects in gelation (**Fig. 3b, bottom**). Circular free-standing features are very difficult to achieve on microfluidic chips with standard methods, but were straightforward to produce by on-chip photolithography. As expected, the diameter of the hydrogel features depended linearly on the dimensions defined by the photo-masks (**Fig. 3c**). There was no significant change in feature dimensions after incubation, suggesting all weakly cross-linked or un-crosslinked material was fully removed during the first rinsing step (**Fig. 3c, right**). Features were obtained reproducibly down to 100 μm, the smallest size tested, in all tests under these conditions.

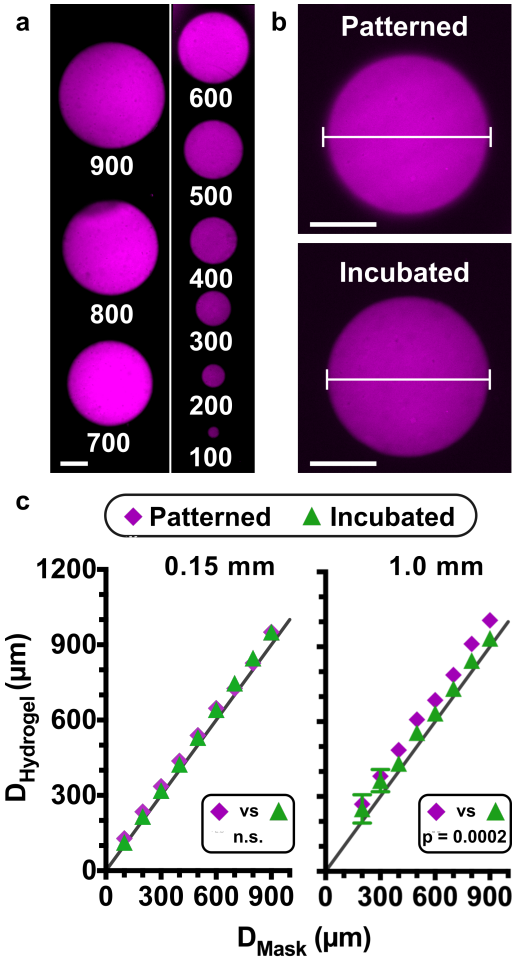

Fig. 3 Assessing Pattern Resolution. (a,b) Fluorescent images of circular hydrogel features (GelSH labelled with NHS-rhodamine) after patterning on a microfluidic chip made with a 0.15-mm coverslip. (a) Features ranged from 900-100 µm in diameter. Scalebar 250 µm. (b) Enlarged images of a representative 600-µm feature immediately after the light exposure and initial rinse ("patterned"), or after a second rinse step following 30-min incubation ("incubated"). White line shows the measurements made. (c) Quantification of accuracy between the diameter of the design on the photomask and the resulting diameter of the hydrogel region after patterning and incubation steps. Plots show hydrogel diameters on microfluidic chips made with (*left*) a 0.15 mm coverslip, n = 4 chips, or (*right*) a 1 mm glass slide, n = 3 chips. Symbols and error bars represent mean and standard deviation; some error bars too small to see. Black line represents y = x. Paired T-test, n.s. indicates $p > 0.05$.

Next, we tested the extent to which resolution was affected by the use of a thicker glass layer (1 mm) for the bottom of the microfluidic device, which is often preferred over coverslips to make more robust chips (**Fig. 3c, right**). Under this condition, while the diameter of the patterned features remained linearly dependent on the dimensions of the photomask, a small corona was formed around the patterns, resulting in larger dimensions. The corona largely disappeared

following incubation, with a significant difference in the size of features after patterning versus incubation indicating the formation of loosely cross-linked materials that later dissolved or were rinsed out. Features were obtained reproducibly down to 200 μm in all tests with the 1 mm glass; 100-μm features did not gel consistently. Therefore, while better resolution and pattern fidelity were obtained with the 0.15 mm coverslip, the more robust chip may be an acceptable tradeoff for applications where larger features are sufficient.

Finally, we tested the robustness of the patterning method to a change in light source. Reproducible gelation absolutely required the use of the collimated light source. Patterning with uncollimated light under the same conditions resulted in inconsistent gelation across chips, in some cases with regions left un-crosslinked, or with features that were weakly cross-linked but washed out after the 30-min incubation period. This phenomenon was consistent with the need for collimation light to provide uniform light intensity during photolithography in other settings, i.e. to mitigate light scattering, interference, and heterogenous dose across the exposed area.

IV. **Photo-crosslinking of free-standing gelatin-based constructs on chip.**

We next tested the extent to which on-chip photolithography provided access to micropatterned hydrogel geometries at increasing levels of complexity. First, we tested the ability to pattern open channels and a curved fluidic path (**Fig. 4a**). By preventing exposure of the precursor solution in the center of the chamber, we were able to pattern two self-standing lobes divided by an open, central channel through which fluid could flow. Next, we tested geometries that are challenging to achieve by standard microfluidic patterning methods. It was straightforward to pattern regions with shared, non-linear boundaries, e.g. by creating a self-standing island followed by a second surrounding hydrogel (**Fig. 4b**). The two regions were visually in contact under microscopic imaging, without a gap. This geometry may be useful for cellular invasion assays or angiogenesis, for example. We extended this system to pattern three sequential regions in concentric circles (**Fig. 4c**). Finally, to test the versatility with more intricate geometries

and alignment capabilities, we recreated the University of Virginia (UVA) historic Rotunda by patterning hydrogels in three sequential steps: 1) the columns, 2) the negative space surrounding the columns, and 3) the dome and foundation (**Fig. 4d**). In all cases, the second and subsequent patterns were achieved through the use of photomasks that covered the previously patterned constructs, ensuring that each region only received one dose of light. We note that these experiments used the same parent microfluidic chamber for all designs; only the photomasks were changed. Thus, the organization was altered rapidly between subsequent devices, without time-consuming master fabrication.

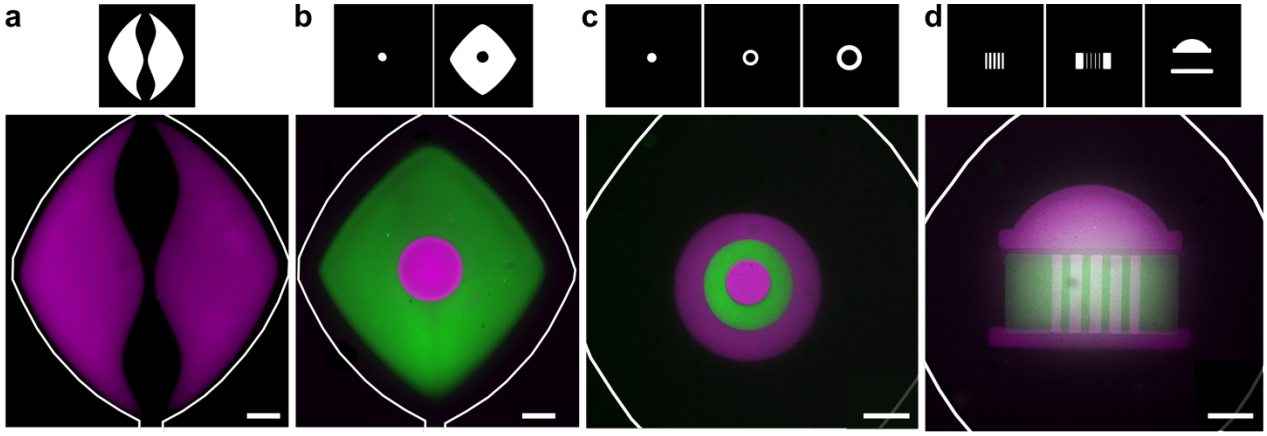

Fig. 4 Geometric versatility achieved by on-chip photo-patterning of GelSH hydrogels. (a) NHS-rhodamine-labelled hydrogel (magenta) used to pattern a curved fluidic path in culture chamber. (b) A central circular island (magenta) surrounded by NHS-fluorescein-labelled GelSH (green). (c) Concentric circles patterned with hydrogel labelled with NHS-rhodamine and NHS-fluorescein in three sequential steps. (d) A patterned UVA Rotunda in three sequential steps. The corresponding photomasks used to achieve patterns are shown above each panel. All scalebars are 500 μm.

V. <u>Photo-crosslinking of free-standing cell-laden gelatin-based constructs on chip</u>

Finally, we tested the ability to directly and cleanly pattern cell-laden features in targeted locations on chip. Primary naïve human T cells (CD4+) were used as a rigorous case study, as these cells are more fragile than cell lines or fibroblastic cells, and are of interest for on-chip

testing of immunotherapies. The T cells were suspended in the precursor solution immediately before loading it onto the chip for patterning. As with the cell-free patterns, the cell-laden un-crosslinked hydrogel was readily washed out from designated open channels in the center and edges of the chamber (**Fig. 5a,b**). Next, we tested the ability to pattern complex, cell-laden geometries with a stylized alien facial pattern. The central eyes and mouth were patterned first, followed by the surrounding head shape (**Fig. 5c,d**). These geometries would be challenging to obtain on-chip by laminar flow or by surface-tension, even with the inclusion of micropillars. The on-chip micropatterning method for 3D cultures was also compatible with additional gelation chemistries, as demonstrated with gelatin norbornene (GelNB) + PEG-thiol linker and gelatin methacryloyl (GelMA) (Fig. S4).

We note that while there is great flexibility to the types of geometries that can be achieved with this method, one is limited by the requirement to rinse out un-crosslinked materials. In particular, concave structures and shapes with voids, such as the letters A and O, are not directly accessible, but multi-step patterning offers a potential solution to this issue. For example, to pattern a cell-laden ring around a cell-free center, the inner region would be patterned first using gel without cells, followed by the surrounding ring.

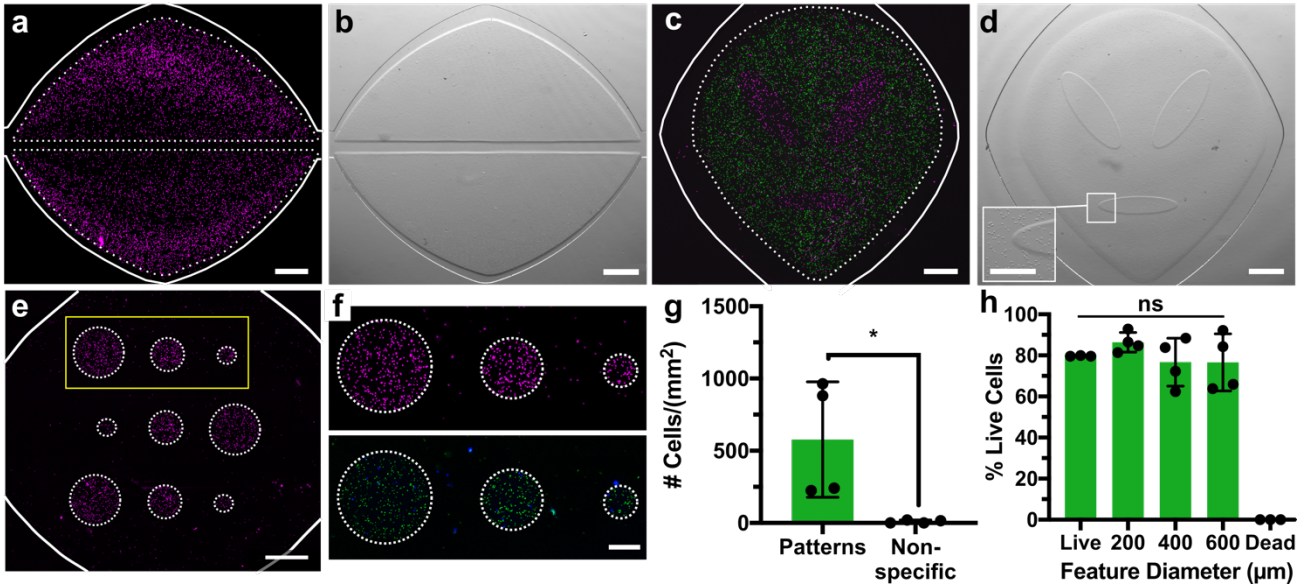

Fig. 5 Cell-laden hydrogel constructs and precision and viability of patterned human T Cells. (a) Fluorescence and (b) brightfield images of a patterned 3D cell culture (cells labelled magenta), patterned into two self-standing lobes. A linear fluidic path was patterned between them, and a second, curved fluidic path surrounded them for better distribution of media. (c) Fluorescence and (d) brightfield image of two distinct cell populations patterned into an alien face geometry. First cell population labelled with NHS-rhodamine (magenta); second population labelled with CFSE (green). Inset shows magnified boundary between two patterned regions. Scalebar is 500 μm in (a-d), 250 μm in inset. Dashed lines denote the boundary of the hydrogel regions; solid white lines indicate the edges of the microfluidic culture chamber. (e) Nine-circle culture array patterned on-chip with cells pre-labelled with NHS-rhodamine. Scalebar 500 μm. (f) Zoomed-in view of area outlined in yellow in panel 5e. (*Top)* Image of NHS-rhodamine labelled cells; (*bottom*) image after viability staining with Calcein-AM (green) and DAPI (blue). Scalebar 200 μm. (g) Quantification of the cell density within the patterned hydrogel regions vs. in non-patterned areas ($p = 0.0293$, unpaired T-test, n=4 chips). (h) Quantification of the viability of patterned CD4+ T cells after 60 - 90 minutes of culture under continuous fluid flow, versus off-chip live controls (ns indicates $p > 0.05$, one-way ANOVA with Tukey's multiple comparisons, n=4 chips). Representative of two independent experiments.

Next, we investigated the spatial precision of cellular patterning. During the loading of the chip, the cell-laden precursor filled the entire culture chamber, giving cells an opportunity to non-specifically adhere to the surfaces of the chip outside the intended patterned regions. To rigorously quantify the specificity of cell location in the patterns, we created an array of 9 circular features per chip in diameters of 200, 400, and 600 μm, and patterned the cells at high density (>

10^7 cells/mL) (**Fig. 5e,f**). As expected, the mean density per unit area in the patterned regions was high, ~ 600 cells/mm^2, and there was minimal cell density in the non-exposed regions, ~ 9 cells/mm^2, or less than 2% of that in intended patterned areas (**Fig. 5g**). These data suggest that non-specific adhesion was minimal outside of patterned hydrogels. The high efficiency of targeted patterning may be the result of the rapid loading and short exposure times, which allowed for the rinsing step to start less than one minute after cells enter the chamber.

Finally, we tested the effects of patterning and pattern geometry on short-term cell survival. The micropatterned GelSH-based cultures from the previous experiment (**Fig. 5e,f**) were cultured for approximately one hour under continuous flow of media to ensure replenishment of nutrients and oxygen. This arrangement allowed us to quickly scan for effects of geometry, since all features were patterned in one chip. We assessed the viability of the cultures by flowing in a Calcein-AM/DAPI (live/dead) staining solution after the culture period (**Fig. 5f, bottom**). Even with these fragile primary cells, there was no significant difference in the percentage of live cells between the feature dimensions, nor between on-chip cultures and off-chip unpatterned controls (**Fig. 5g**), indicating that the patterning method was cytocompatible. Similarly, cultures patterned in GelNB using primary murine splenocytes also retained high viability, 85% of that of controls, whereas patterns in GelMA had variable viability, trending towards lower values (~70% of that of controls) (Fig. S4b,c), consistent with prior reports.[41] Thus, on-chip micropatterning of sensitive cell types may be best generated using norbornene-thiol chemistry, while methacryloyl chemistry may be restricted to hardier cell types. Future work will focus in exploring any effects of this patterning method on long-term cell cultures.

Conclusion

In summary, we describe a method for in situ micropatterning of spatially organized biomaterials and 3D cell cultures on a microfluidic chip. The method was demonstrated with three different photo-reactive chemistries, indicating versatility and robustness. By simply aligning a

photomask prior to blue light exposure, the user may pattern a wide variety of design configurations in the xy-plane without altering the microfluidic housing. The resulting patterned cultures were highly modular and free-standing, which eliminates the need for physical supports like micropillars in order to guide the hydrogel in place. Geometries such as concentric circles, architectural designs, and microarrays were all accessible, as were open flow paths to distribute media to the patterned 3D cultures. When used with norbornene-thiol gelation chemistry, the micropatterning method had low cytotoxicity with fragile primary cells. We envision this micropatterning strategy will enable researches to organize 3D cultures directly onto microfluidic chips in arrangements that capture the complexity of tissue organization and grant access to mechanistic experiments while maintaining control over cellular and fluidic components.

MATERIALS & METHODS

GelSH Matrix Characterization

Thiol-modified gelatin (GelSH; Lot: MKCJ5413) was obtained from Sigma Aldrich with a vendor-reported absolute degree of functionalization of 0.223 mmol -SH / g gelatin, as determined by free thiol assay, and used as provided. 8-arm PEG-NB 20 kDa (Jenkem Technologies) and lithium phenyl-2,4,6-trimethylbenzoylphosphinate (LAP; Sigma Aldrich) were also used as provided. For rheological measurements, the precursor solution was prepared by combining reagents to a final concentration of 5% w/v GelSH, 10 or 20 mM norbornene (1.25 or 2.5 mM PEG-NB linker), and 3.4 mM LAP in 1x phosphate buffered saline without calcium or magnesium (PBS; Lonza). Rheological characterization was performed using a MCT302 Anton Parr Rheometer, operated in oscillatory time sweep mode with 5% strain, 1 Hz frequency, and 0.1 mm gap to assess gel polymerization rate and storage modulus. A UV-curing stage was fitted with a 20-mm parallel plate, the light source was filtered through a 400-500 nm filter, and the stage temperature was maintained at 25 ^{o}C. 30 μL of precursor solution was pipetted onto the stage.

After measuring baseline stiffness for 30 seconds, light exposure at 50 mW/cm^2 was initiated and continued until a phase transition was observed and the resulting solid reached a constant stiffness (~2 min).

Microfluidic Device Fabrication and Surface Modification

A two-layer microfluidic device was fabricated using standard soft lithography methods. Transparency masks were drawn in AutoCAD LT 2019 and printed at 20,000 DPI by CAD/Art Services, Inc. (Brandon, OR). The master molds were fabricated using SU-8 3050 photoresist spun to 124 – 136 µm thickness (Microchem, Westborough MA, USA) on 3" silicon wafers (University Wafer, South Boston MA, USA) and vapor silanized with Trichloro(1*H*,1*H*,2*H*,2*H*-perfluorooctyl) silane (Sigma Aldrich) for 2 hours. Degassed polydimethylsiloxane (PDMS) was prepared at a 10:1 ratio of elastomer base to curing agent (Slygard 184 Silicone Elastomer, Ellsworth Adhesives, Germantown WI, USA), poured over the silicon SU-8 master, and cured in a 70 ºC oven for at least 2 hours.

Once cured, the PDMS was removed from the master and punched at the channel ends using a 0.75-mm I.D. tissue punch (World Precision Instruments, Sarasota FL, USA) to create inlets for PFTE TT-30 tubing (Weico Wire Inc.). The PDMS layer and a Goldseal cover glass (35 x 50 mm x 0.15 mm, actual thickness 0.13-0.16 mm, Ted Pella, Inc.) were oxidized in plasma cleaner for 20 seconds (air plasma; Tegal Plasmod), manually assembled, and incubated in a 120 ºC oven for 10 minutes to complete the bonding process. Where noted, a ~ 1 mm thick Corning® Glass Slides, 75 x 50 mm (Ted Pella, Inc.) was used instead of the glass coverslip. The device was then purged with nitrogen for 10 min, followed by 90 min of vapor silanization using (3-Mercaptopropyl) trimethoxy silane (Sigma Aldrich) in a nitrogen-filled environment. For devices to be used with GelMA, 3-(Trimethoxysilyl)propyl methacrylate (Sigma Aldrich) was used instead. After silanization, the device was rinsed with 70% ethanol and distilled water, purged with a nitrogen gun to remove excess moisture, and placed in a 120 ºC oven to dry completely for at

least 10 min. Once dried, the device was covered with tape to prevent dust accumulation and stored in a desiccator containing Dri-rite. Devices were used within a week of being silanized.

A rigid poly(methyl methacrylate) (PMMA) cover was fabricated to serve as a backing for the photomask. To avoid light scattering or absorption during photo-crosslinking, a hole was cut into the PMMA over the culture chamber. Specifically, a 50 x 45 x 1.5 mm acrylic sheet (McMaster-Carr, Princeton, NJ USA) was etched with a 10-mm central hole by using a CO_2 laser (Versa Laser 3.5, Universal Laser System, Scottsdale, AZ) set to 20% power and 1% speed.

Photo-patterning of spatially organized hydrogels and 3D cultures on chip

Prior to photopatterning, a precursor solution was prepared by combining reagents to a final concentration of 5% GelSH and 3.4 mM LAP in 1x PBS. This solution was stored at 4 ºC overnight before use. In some cases, the GelSH was fluorescently labelled prior to gelation by pipetting a reactive dye into the precursor solution and vortexing for 30 seconds at room temperature. Final concentrations of reactive dye were 5 μM NHS-rhodamine, 53 μM NHS-fluorescein, or 31 μM Alexa Fluor 594-succinimidyl ester (ThermoFisher). For experiments with cells, the cells were centrifuged at 400 x g for 5 min to remove culture media, resuspended in 1x PBS, and centrifuged again to remove 1x PBS immediately before resuspending in precursor solution. PEG-NB linker was added to a final concentration of 1.25 mM immediately before loading the precursor solution into syringes.

The microfluidic chip was sterilized with 70% ethanol for 2.5 min, followed by a 5 min rinse with DI water and a subsequent 5 min rinse with 1x PBS, all at 5 μL/min. All rinse steps were performed by using a Chemyx syringe pump (Fusion 200, Houston TX, USA) and a 1-mL Hamilton™ Gastight Microliter™ syringe. Precursor solution was flowed into the chip for 2 min at 5 μL/min, and a 25-μL Hamilton™ 700/1700 Series Gastight™ syringe and TT-30 tubing (Weico Wire). The inlets and outlets were blocked off with PDMS-filled TT-30 tubing to prevent air entry. Next, the chip was placed on an aluminum cooling plate with a reusable ice pack (Dulytek,

Amazon) at 14 – 18 ºC for 45 seconds to cool the device; this step ensured a consistent temperature across chips during gelation. The photo-mask was taped to the PMMA cover, aligned to the coverslip of the chip, and clamped using binder clips. The chip was then overturned and exposed to light using a Fiber Coupled Violet LED light source at 405 nm (±5 nm) attached to a Ø0.5 inch fiber collimator (Prizmatix, Inc., Israel). The light intensity was set to 50 mW/cm^2 and the chip exposed for 45 sec to achieve the optimized dose of 2.25 J/cm^2, unless otherwise noted. Once patterned, the device was returned to its upright position and rinsed with room temp 1x PBS for 5 min at 5 µL/min. If additional patterning steps were necessary, device was re-loaded with a new precursor solution, cooled, aligned, exposed, and rinsed. Finally, for experiments where cells were present, appropriate culture media was flowed in for 2 min at 5 µL/min before the chip was connected to perfusion at lower flow rate either via syringe or peristaltic pump.

Widefield Imaging

All imaging was performed on an upright AxioZoom macroscope using an HXP 200C metal halide lamp, PlanNeoFluor Z 1x/0.25 FWD 56 mm objective, and Axiocam 506 mono camera (Carl Zeiss Microscopy). For fluorescence imaging, filters used were Zeiss Filter Set 38 HE (Ex: 470/40, Em: 525/50), 43 HE (Ex: 550/25, Em: 605/70); 64 HE (Ex: 587/25, Em: 647/70); and 49 HE (Ex: 365, Em: 445/50). Brightfield images were collected using transmitted light. Zen 2 Blue software was used for image collection, and images were analyzed in ImageJ v1.52k.

Assessing Patterning Resolution

Chips were assembled as described above, with the bottom layer comprised of either a coverslip (0.13 – 0.16 mm thickness) or a 1-mm thick Corning® Glass Slides, 75 x 50 mm (Ted Pella, Inc.). A precursor solution composed of 5% GelSH, 1.25 mM PEG-NB linker, 3.4 mM LAP, and 5 µM NHS-Rhodamine was patterned on-chip as described above, using a 45 second exposure at 50 mW/cm^2. Un-crosslinked material was rinsed out with 1x PBS for 5 min at 5 µL/min,

after which the inlet and outlet were closed using TT-30 (Weico Wire) tubing filled with PDMS. The chips were placed in an incubator (37 ºC, 5% CO_2) for 30 minutes in the absence of flow, then chips rinsed once more with 1x PBS for 5 minutes at 5 µL/min. Features were imaged by brightfield and fluorescence microscopy on a Zeiss AxioZoom microscope (HE 43 filter set). The diameter of each feature was quantified from the fluorescence images by using line tools in ImageJ v1.52k.

Photopatterning and analysis of human lymphocytes (GelSH)

Human naïve CD4+ T cells were purified from TRIMA collars, a byproduct of platelet apheresis, obtained from healthy donors (INOVA Laboratories; Sterling, VA). Initially, total CD4+ T cells were isolated using a combination of the human CD4+ T cell RosetteSep™ kit (STEMCELL Technologies) and Ficoll-Paque (Cytiva Inc.) density centrifugation. Naïve CD4+ T cells were then enriched from total CD4+ T cells through immuno-magnetic negative selection with the EasySep™ Naïve CD4+ T cell isolation kit (STEMCELL Technologies). Naïve CD4+ T cell post-isolation purity (CD4+CD45RA+CD45RO-) was determined through flow cytometry (Fig. S3). Cells were labelled using 10 µM NHS-rhodamine for 20 min at room temperature, rinsed in 1x PBS to remove excess dye by centrifugation at 400 x g for 5 min and resuspended in AIM V serum-free medium (Gibco; Thermo Fisher Scientific, Inc.) supplemented with 10 ng/mL recombinant human IL-7 (R&D Systems; Bio-techne, Inc.) until use.

For micropatterning, cells were resuspended in precursor solution at 1.25 x 10^7 cells/mL. The 8 arm PEG-NB was added to the precursor to a final concentration of 1.25 mM immediately before filling the syringe. Cells were flowed into the device for 2 min at 5 µL/min and photo-patterned as described above. Micropatterned cultures were incubated in a cell culture incubator (37 ºC, 5% CO_2) for 60 - 90 min under continuous perfusion of media (AIM-5, supplemented with 10 ng/mL recombinant human IL-7) at 0.8 µL/min. Media perfusion was controlled by using an Ismatec IPC-N ISM937C Digital Peristaltic Pump (Cole Palmer, Inc.) and LMT-55 tubing (I.D. 0.25

mm; Cole Palmer, Inc.), which was connected to TT-30 tubing (Weico Wire) to make a direct connection to the inlet of the device.

After the culture period, the viability of cells was assessed by flowing in a staining solution of Calcein-AM (5 μM) and DAPI (1 μM) in 1x PBS for 2 min at 5 μL/min, which was incubated on-chip for 20 min at 37 ^{o}C, then rinsed out for 10 min with 1x PBS at 5 μL/min using a syringe pump. Images were collected using a Zeiss AxioZoom microscope, collecting two to four focal planes per location. Data analysis was performed in ImageJ, as follows: The z-stack images from each location were stacked and converted into a Max Intensity Projection. Cells were identified by using the Particle Analyzer tool (circularity 0.5 – 1, size 12.5 – 500 μm^2). The percent of live cells was quantified as Calcein-positive cells/ (Calcein-positive + DAPI-positive cells).

To quantify cell density inside and outside of the patterned structures, images were analyzed using ImageJ. Cells were identified by using the Particle Analyzer tool (circularity 0.5 – 1, size 12.5 – 500 μm^2). Cell density was calculated as the number of cells per unit area (mm^2), by selectively analyzing the area inside of all hydrogel features and the negative space in the chamber outside of the features.

Synthesis and characterization of GelMA and GelNB

GelNB was synthesized as described by Mũnoz et al., (2014).[41] In summary, an aqueous solution of type A porcine gelatin (Sigma Aldrich) was brought to 3.7 mM carbic anhydride (Sigma Aldrich) and stirred for 72 hours at 50 ^{o}C while a pH of 8 was maintained with pellets of sodium hydroxide (Avantor Performance Materials.) The reaction mixture was then centrifuged at 3500 x g for 3 minutes and the supernatant was dialyzed against DI water at 40 ^{o}C for 10 days. The resulting protein solution was adjusted to have a pH of 7.4, filtered, lyophilized, and stored at -20 ^{o}C until needed.

GelMA was synthesized as described by Loessner et al. (2016).[53] Methacrylic anhydride (MA; Sigma Aldrich) was added to type A porcine gelatin at a 13 mmol MA / g gelatin ratio and

stirred for 1 hour at 50 °C. The reaction was centrifuged at 3500 x g for 3 minutes and the supernatant was dialyzed against DI water at 40 °C for 10 days. The protein solution was then adjusted to have a pH of 7.4, filtered, lyophilized, and stored at -20 °C until needed.

The absolute and fractional functionalization of the GelNB and GelMA were determined using ^{1}H-NMR and an optimized ninhydrin assay for functionalized gelatin as described by Zatorski, et al., (2020).[54] GelNB and GelMA had a fractional degree of functionalization of 65-70% and 55-65%, respectively, as determined by the ninhydrin assay.

Photopatterning and analysis of murine splenocytes (GelMA and GelNB)

All animal work was approved by the Animal Care and Use Committee of the University of Virginia under protocol #4042, and was conducted in compliance with guidelines from the University of Virginia Animal Care and Use Committee and the Office of Laboratory Animal Welfare at the National Institutes of Health (United States). Mice were housed in a vivarium and given food and water *ab libitium*. Spleens were collected from male and female C57Bl/6 mice aged 8–12 weeks (Jackson Laboratories, USA) after isoflurane anesthesia and cervical dislocation. To isolate splenocytes, the spleen was processed through a 70-µm pore size nylon filter (Fisher Scientific, USA) and rinsed with sterile 1x PBS supplemented with 2% v/v fetal bovine serum (FBS, VWR, USA). Red blood cells were lysed and the cell suspension was filtered through a fresh 70-µm filter and resuspended in “complete RPMI media”: RPMI (Lonza, 16-167F) supplemented with 10 % FBS (VWR, Seradigm USDA approved, 89510-186), 1x L-glutamine (Gibco Life Technologies, 25030-081), 50 U/mL Pen/Strep (Gibco), 50 µM betamercaptoethanol (Gibco, 21985-023), 1 mM sodium pyruvate (Hyclone, GE USA), 1x non-essential amino acids (Hyclone, SH30598.01), and 20 mM HEPES (VWR, 97064-362). Cells were cultured in this media until ready for use. “Killed” controls were generated by resuspending cells in 70% ethanol for 10 minutes, then resuspending in media until use.

For patterning in GelMA, a precursor solution was prepared to a final concentration of 10% GelMA and 3.4 mM LAP photoinitiator in 1x PBS. Photo-patterning occurred as described above, with cells resuspended at $1x10^7$/mL in the precursor solution, with an exposure time of 60 sec at 50 mW/cm^2. For patterning in GelNB, a precursor solution was prepared to a final concentration of 5% GelNB, 3.75 mM 4-arm 5 kDa PEG-thiol (Jenkem Technologies), and 3.4 mM LAP in 1x PBS. Photo-patterning occurred as described above, with an exposure time of 60 sec at 50 mW/cm^2. Chips were incubated (37 ºC, 5% CO_2) for 1 hour under continuous flow of complete RPMI media, using a Chemyx Fusion 200 syringe pump at 5 µL/min. After the culture period, cells were stained with 5 µM Calcein AM and 5 µM Propidium Iodide for 20 min, rinsed with PBS for 5 min, and imaged with a Zeiss AxioZoom microscope. Data was analyzed as described above to determine viability.

Statistical Analysis

Statistical tests and curve fits were performed in GraphPad Prism 8.4.3.

Conflict of Interest Statement

The authors have no conflicts to declare.

Acknowledgments

The authors would like to thank the Lampe lab for early feedback, providing LAP photoinitiator, and access to their lyophilizer, and the Landers lab for access to the CO_2 laser etcher. We would like to also thank the UVA Center for Advanced Biomanufacturing (CAD Bio) for access to the rheometer and the Caliari lab for training and access to the lyophilizer equipment. This work was supported by a seed award from the CAD Bio Center, and by the National Institute of Biomedical Imaging and Bioengineering (NIBIB) under Award Number U01EB029127 through the National Institutes of Health (NIH), with co-funding from the National Center for Advancing

Translational Sciences (NCATS). JOC was supported in part by the NIH-funded T32 Biotechnology Training Program at the University of Virginia. JMZ was supported in part by the Graduate Research Fellowship Program through the National Science Foundation. ANM was supported in part by the Harrison Undergraduate Research Award through the Office of Undergraduate Research (OUR) Grant at the University of Virginia.

References:

1 D'Arcangelo E, McGuigan AP. Micropatterning strategies to engineer controlled cell and tissue architecture in vitro. *BioTechniques* 2015; **58**: 13–23.

2 Tenje M, Cantoni F, Porras Hernández AM, Searle SS, Johansson S, Barbe L *et al.* A practical guide to microfabrication and patterning of hydrogels for biomimetic cell culture scaffolds. *Organs---Chip* 2020; **2**: 100003.

3 Ayuso JM, Virumbrales-Muñoz M, Lacueva A, Lanuza PM, Checa-Chavarria E, Botella P *et al.* Development and characterization of a microfluidic model of the tumour microenvironment. *Sci Rep* 2016; **6**. doi:10.1038/srep36086.

4 Lesher-Perez SC, Kim G-A, Kuo C, Leung BM, Mong S, Kojima T *et al.* Dispersible oxygen microsensors map oxygen gradients in three-dimensional cell cultures. *Biomater Sci* 2017; **5**: 2106–2113.

5 Aleman J, George SK, Herberg S, Devarasetty M, Porada CD, Skardal A *et al.* Deconstructed Microfluidic Bone Marrow On-A-Chip to Study Normal and Malignant Hemopoietic Cell–Niche Interactions. *Small* 2019; **15**: 1902971.

6 Rajan SAP, Skardal A, Hall AR. Multi-Domain Photopatterned 3D Tumor Constructs in a Micro-Physiological System for Analysis, Quantification, and Isolation of Infiltrating Cells. *Adv Biosyst* 2020; **4**: e1900273.

7 Wylie RG, Ahsan S, Aizawa Y, Maxwell KL, Morshead CM, Shoichet MS. Spatially controlled simultaneous patterning of multiple growth factors in three-dimensional hydrogels. *Nat Mater* 2011; **10**: 799–806.

8 Han S, Yan J-J, Shin Y, Jeon JJ, Won J, Jeong HE *et al.* A versatile assay for monitoring in vivo-like transendothelial migration of neutrophils. *Lab Chip* 2012; **12**: 3861–3865.

9 Hu X, Zhao S, Luo Z, Zuo Y, Wang F, Zhu J *et al.* On-chip hydrogel arrays individually encapsulating acoustic formed multicellular aggregates for high throughput drug testing. *Lab Chip* 2020; **20**: 2228–2236.

10 Tewary M, Dziedzicka D, Ostblom J, Prochazka L, Shakiba N, Heydari T *et al.* High-throughput micropatterning platform reveals Nodal-dependent bisection of peri-gastrulation–associated versus preneurulation-associated fate patterning. *PLOS Biol* 2019; **17**: e3000081.

11 Park D, Son K, Hwang Y, Ko J, Lee Y, Doh J *et al.* High-Throughput Microfluidic 3D Cytotoxicity Assay for Cancer Immunotherapy (CACI-IMPACT Platform). *Front Immunol* 2019; **10**. doi:10.3389/fimmu.2019.01133.

12 Offenhäusser A, Böcker-Meffert S, Decker T, Helpenstein R, Gasteier P, Groll J *et al.* Microcontact printing of proteins for neuronal cell guidance. *Soft Matter* 2007; **3**: 290–298.

13 Qin D, Xia Y, Whitesides GM. Soft lithography for micro- and nanoscale patterning. *Nat Protoc* 2010; **5**: 491–502.

14 Ouyang A, Cerchiari AE, Tang X, Liebenberg E, Alliston T, Gartner ZJ *et al.* Effects of cell type and configuration on anabolic and catabolic activity in 3D co-culture of mesenchymal stem cells and nucleus pulposus cells. *J Orthop Res* 2017; **35**: 61–73.

15 Lee UN, Day JH, Haack AJ, Bretherton RC, Lu W, DeForest CA *et al.* Layer-by-layer fabrication of 3D hydrogel structures using open microfluidics. *Lab Chip* 2020; **20**: 525–536.

16 Miri AK, Mostafavi E, Khorsandi D, Hu S-K, Malpica M, Khademhosseini A. Bioprinters for organs-on-chips. *Biofabrication* 2019; **11**: 042002.

17 Miri AK, Nieto D, Iglesias L, Goodarzi Hosseinabadi H, Maharjan S, Ruiz-Esparza GU *et al.* Microfluidics-Enabled Multimaterial Maskless Stereolithographic Bioprinting. *Adv Mater* 2018; **30**: 1800242.

18 Yanagawa F, Sugiura S, Kanamori T. Hydrogel microfabrication technology toward three dimensional tissue engineering. *Regen Ther* 2016; **3**: 45–57.

19 E. Brown T, S. Anseth K. Spatiotemporal hydrogel biomaterials for regenerative medicine. *Chem Soc Rev* 2017; **46**: 6532–6552.

20 Takeuchi M, Kozuka T, Kim E, Ichikawa A, Hasegawa Y, Huang Q *et al.* On-Chip Fabrication of Cell-Attached Microstructures using Photo-Cross-Linkable Biodegradable Hydrogel. *J Funct Biomater* 2020; **11**. doi:10.3390/jfb11010018.

21 Sato K, Kikuchi S, Yoshida E, Ishii R, Sasaki N, Tsunoda K *et al.* Patterned Co-culture of Live Cells on a Microchip by Photocrosslinking with Benzophenone. *Anal Sci* 2016; **32**: 113–116.

22 Zhu M, Wang Y, Ferracci G, Zheng J, Cho N-J, Lee BH. Gelatin methacryloyl and its hydrogels with an exceptional degree of controllability and batch-to-batch consistency. *Sci Rep* 2019; **9**: 6863.

23 Skardal A, Devarasetty M, Soker S, Hall AR. In situ patterned micro 3D liver constructs for parallel toxicology testing in a fluidic device. *Biofabrication* 2015; **7**: 031001.

24 Aung A, Kumar V, Theprungsirikul J, Davey SK, Varghese S. An Engineered Tumor-on-a-Chip Device with Breast Cancer–Immune Cell Interactions for Assessing T-cell Recruitment. *Cancer Res* 2020; **80**: 263–275.

25 LeValley PJ, Noren B, Kharkar PM, Kloxin AM, Gatlin JC, Oakey JS. Fabrication of Functional Biomaterial Microstructures by in Situ Photopolymerization and Photodegradation. *ACS Biomater Sci Eng* 2018; **4**: 3078–3087.

26 Lampi MC, Guvendiren M, Burdick JA, Reinhart-King CA. Photopatterned Hydrogels to Investigate the Endothelial Cell Response to Matrix Stiffness Heterogeneity. *ACS Biomater Sci Eng* 2017; **3**: 3007–3016.

27 Gurkan UA, Fan Y, Xu F, Erkmen B, Urkac ES, Parlakgul G *et al.* Simple Precision Creation of Digitally Specified, Spatially Heterogeneous, Engineered Tissue Architectures. *Adv Mater* 2013; **25**: 1192–1198.

28 Peela N, Sam FS, Christenson W, Truong D, Watson AW, Mouneimne G *et al.* A three dimensional micropatterned tumor model for breast cancer cell migration studies. *Biomaterials* 2016; **81**: 72–83.

29 Davey SK, Aung A, Agrawal G, Lim HL, Kar M, Varghese S. Embedded 3D Photopatterning of Hydrogels with Diverse and Complex Architectures for Tissue Engineering and Disease Models. *Tissue Eng Part C Methods* 2015; **21**: 1188–1196.

30 Therriault D, White SR, Lewis JA. Chaotic mixing in three-dimensional microvascular networks fabricated by direct-write assembly. *Nat Mater* 2003; **2**: 265–271.

31 Annabi N, Selimović Š, Cox JPA, Ribas J, Bakooshli MA, Heintze D *et al.* Hydrogel-coated microfluidic channels for cardiomyocyte culture. *Lab Chip* 2013; **13**: 3569–3577.

32 Rosa PM, Gopalakrishnan N, Ibrahim H, Haug M, Halaas Ø. The intercell dynamics of T cells and dendritic cells in a lymph node-on-a-chip flow device. *Lab Chip* 2016; **16**: 3728–3740.

33 Kim HJ, Du W, Ismagilov RF. Complex Function by Design Using Spatially Pre-Structured Synthetic Microbial Communities: Degradation of Pentachlorophenol in the Presence of Hg(II). *Integr Biol Quant Biosci Nano Macro* 2011; **3**: 126–133.

34 Bang S, Lee S-R, Ko J, Son K, Tahk D, Ahn J *et al.* A Low Permeability Microfluidic Blood-Brain Barrier Platform with Direct Contact between Perfusable Vascular Network and Astrocytes. *Sci Rep* 2017; **7**: 8083.

35 Ebrahimi M, Ostrovidov S, Salehi S, Kim SB, Bae H, Khademhosseini A. Enhanced skeletal muscle formation on microfluidic spun gelatin methacryloyl (GelMA) fibres using surface patterning and agrin treatment. *J Tissue Eng Regen Med* 2018; **12**: 2151–2163.

36 Panda P, Ali S, Lo E, Chung BG, Hatton TA, Khademhosseini A *et al.* Stop-Flow Lithography to Generate Cell-Laden Microgel Particles. *Lab Chip* 2008; **8**: 1056–1061.

37 Jiang Z, Shaha R, McBride R, Jiang K, Tang M, Xu B *et al.* Crosslinker length dictates step-growth hydrogel network formation dynamics and allows rapid on-chip photoencapsulation. *Biofabrication* 2020; **12**: 035006.

38 Van Hoorick J, Tytgat L, Dobos A, Ottevaere H, Van Erps J, Thienpont H *et al.* (Photo-)crosslinkable gelatin derivatives for biofabrication applications. *Acta Biomater* 2019; **97**: 46–73.

39 McCall JD, Anseth KS. Thiol–Ene Photopolymerizations Provide a Facile Method To Encapsulate Proteins and Maintain Their Bioactivity. *Biomacromolecules* 2012; **13**: 2410–2417.

40 Greene T, Lin C-C. Modular Cross-Linking of Gelatin-Based Thiol–Norbornene Hydrogels for in Vitro 3D Culture of Hepatocellular Carcinoma Cells. *ACS Biomater Sci Eng* 2015; **1**: 1314–1323.

41 Mũnoz Z, Shih H, Lin C-C. Gelatin hydrogels formed by orthogonal thiol–norbornene photochemistry for cell encapsulation. *Biomater Sci* 2014; **2**: 1063–1072.

42 Gould ST, Darling NJ, Anseth KS. Small Peptide Functionalized Thiol-Ene Hydrogels as Culture Substrates for Understanding Valvular Interstitial Cell Activation and de novo Tissue Deposition. *Acta Biomater* 2012; **8**: 3201–3209.

43 Liu H-Y, Korc M, Lin C-C. Biomimetic and enzyme-responsive dynamic hydrogels for studying cell-matrix interactions in pancreatic ductal adenocarcinoma. *Biomaterials* 2018; **160**: 24–36.

44 Nichol JW, Koshy ST, Bae H, Hwang CM, Yamanlar S, Khademhosseini A. Cell-laden microengineered gelatin methacrylate hydrogels. *Biomaterials* 2010; **31**: 5536–5544.

45 Van Hoorick J, Gruber P, Markovic M, Rollot M, Graulus G-J, Vagenende M *et al.* Highly Reactive Thiol-Norbornene Photo-Click Hydrogels: Toward Improved Processability. *Macromol Rapid Commun* 2018; **39**: e1800181.

46 Fairbanks BD, Schwartz MP, Bowman CN, Anseth KS. Photoinitiated polymerization of PEG-diacrylate with lithium phenyl-2,4,6-trimethylbenzoylphosphinate: polymerization rate and cytocompatibility. *Biomaterials* 2009; **30**: 6702–6707.

47 Murphy MC, Iii JH, Jr CRJ, Glaser KJ, Senjem ML, Chen J *et al.* Measuring the Characteristic Topography of Brain Stiffness with Magnetic Resonance Elastography. *PLOS ONE* 2013; **8**: e81668.

48 de la Zerda A, Kratochvil MJ, Suhar NA, Heilshorn SC. Review: Bioengineering strategies to probe T cell mechanobiology. *APL Bioeng* 2018; **2**: 021501.

49 Purwada A, Jaiswal MK, Ahn H, Nojima T, Kitamura D, Gaharwar AK *et al.* Ex vivo engineered immune organoids for controlled germinal center reactions. *Biomaterials* 2015; **63**: 24–34.

50 Regehr KJ, Domenech M, Koepsel JT, Carver KC, Ellison-Zelski SJ, Murphy WL *et al.* Biological implications of polydimethylsiloxane-based microfluidic cell culture. *Lab Chip* 2009; **9**: 2132–2139.

51 Pereiro I, Khartchenko AF, Petrini L, Kaigala GV. Nip the bubble in the bud: a guide to avoid gas nucleation in microfluidics. *Lab Chip* 2019; **19**: 2296–2314.

52 Bowden N, Huck WTS, Paul KE, Whitesides GM. The controlled formation of ordered, sinusoidal structures by plasma oxidation of an elastomeric polymer. *Appl Phys Lett* 1999; **75**: 2557–2559.

53 Loessner D, Meinert C, Kaemmerer E, Martine LC, Yue K, Levett PA *et al.* Functionalization, preparation and use of cell-laden gelatin methacryloyl–based hydrogels as modular tissue culture platforms. *Nat Protoc* 2016; **11**: 727–746.

54 Zatorski JM, Montalbine AN, Ortiz-Cárdenas JE, Pompano RR. Quantification of fractional and absolute functionalization of gelatin hydrogels by optimized ninhydrin assay and 1H NMR. *Anal Bioanal Chem* 2020; **412**: 6211–6220.